IEEE Access
Multidisciplinary | Rapid Review | Open Access Journal

Received March 13, 2022, accepted April 2, 2022, date of publication April 7, 2022, date of current version April 18, 2022.

Digital Object Identifier 10.1109/ACCESS.2022.3165645

Reference Model Control of the Time Delayed Double Integrator

MIKULAS HUBA[1], (Member, IEEE), DAMIR VRANCIC[2], AND PAVOL BISTAK[1]

[1]Faculty of Electrical Engineering and Information Technology, Institute of Automotive Mechatronics, Slovak University of Technology in Bratislava, 812 19 Bratislava, Slovakia

[2]Department of Systems and Control, Jožef Stefan Institute, 1000 Ljubljana, Slovenia

Corresponding author: Mikulas Huba (mikulas.huba@stuba.sk)

This work was supported in part by the following grants: ''Advancing University Capacity and Competence in Research, Development and Innovation'' (ITMS project code: 313021X329) supported by Operational Programme Integrated Infrastructure and funded by the European Regional Development Fund; ''Control and modelling of mechatronic systems in emobility'' (No.: 1/0745/19) financed by the Slovak Scientific Agency (VEGA); and within research program P2-0001, financed by the Slovenian Research Agency.

ABSTRACT This paper illustrates the reference model-based dead-time compensator (RM-DTC) recently developed for first-order time-delayed systems using a real-time example, and extends this novel approach for a time-delayed double integrator system. RM-DTC enables fully decoupled setpoint tracking and disturbance reconstruction and compensation. The overall structure of RM-DTC includes feedforward control using either a transfer function based implementation or the primary loop which produces a filtered inverse of the model transfer function. The setpoint feedforward is complemented by a disturbance-observer-based input disturbance reconstruction that also uses the filtered inverse of the plant model. The reference models of setpoint and input disturbance feedforward control allow the introduction of a stabilising PD controller without compromising the nominally independent dynamics of setpoint tracking and disturbance rejection. The main advantage of retaining the full functionality of disturbance reconstruction in RM-DTC is that it enables monitoring and diagnostics of the controlled process, which is important in terms of full automation of running processes representing the fundamental goal of the Industry 4.0 campaign. This surpasses the approaches based on internal model control, which have been modified for unstable systems to achieve internal stability by eliminating the reconstructed disturbance signal from the control loop. The excellent properties of RM -DTCs are illustrated by simulation and real-time control of thermal process.

INDEX TERMS Reference model, time-delayed system, double integrator, dead-time compensator, PID control.

I. INTRODUCTION

In mechatronics, the model of a double integrator representing the motion of physical bodies plays a central role in position control, whether in high-speed positioning control, robotic arms and manipulators, high-performance servo systems, pneumatic muscle actuators, control of electrical vehicles, robot-aided upper limb rehabilitation, flying vehicles, magnetic levitation, etc. (see, for example [1]–[7]). Chains of integrators also appear in the design of nonlinear systems by feedback linearization [8]. In order to obtain an optimal tuning that fully exploits the capabilities of the control loop, it must be supplemented by the time delays, which are usually represented by a dead time element. This then leads to a double integrator plus dead time (DIPDT) model.

Even today, due to the specifics of the applications, such as nonlinear properties (control constraints, friction, hysteresis, quantization), measurement noise, robustness, and computational complexity, we need a variety of different control approaches. The latter is particularly important due to the growing number of applications based on embedded controllers. Therefore, it is still important to search for new approaches and compare them with the traditional ones.

Recently, Grimhold and Skogestad [9] discovered that by constructing a PID controller according to the DIPDT model, it can be successfully used for a variety of dynamical systems. However, such observations are far from unique and do not only concern PID controllers. Among the large number of controllers based on DIPDT models, the discrete-time

The associate editor coordinating the review of this manuscript and approving it for publication was Azwirman Gusrialdi.

solutions with dead-beat performance can be highlighted as examples of "time-optimal" control, first described and applied in [10], to design constrained controllers with anti-windup integral action for stable and unstable, possibly higher-order plants. They were obtained by combining one of the first dead-time compensators (DTCs), based on the reconstruction and compensation of input disturbances by an extended state observer (ESO), with a generalization of the famous method for controller tuning by Ziegler and Nichols [11]. Similar in several aspects to [10], the constrained control of a double integrator was the basis of a special *fhan* function developed by Han [12] and used in combination with the reconstruction and compensation of equivalent disturbances by a state approach with an extended state observer (ESO). This approach, proposed as an alternative to the traditional PID controllers, has been called active disturbance rejection control (ADRC) and in the linear setup denoted also as LADRC has been widely popularized by Gao [13]–[16]. The need to consider the influence of dead time was later incorporated in the LADRC solutions suitable for time-delayed systems [17], [18]. Another similar approach, referred to as model-free control (MFC), based on finite impulse response filters (FIR), was developed by Flies [19], [20]. However, the double integrator models were used even earlier. The time-optimal control algorithms applied to the double integrator for controlling some nonlinear systems were already used by Feldbaum [21], who cites a 1935 patent for rolling mill control with quadratic feedback, which is a typical example of a relay time optimal double integrator control.

It is therefore not surprising that in addition to the aforementioned ADRC and MFC, DIPDT models also play a central role in various PID [22]–[24], or disturbance observer (DOB) control structures [25]–[28]. The slowest penetration of integrating models for modelling and control is seen in the area of Internal Model Control (IMC), which relies on the properties of the Smith predictor (SP) [29]. SP represents the best known structure for the control of time-delayed systems by combining the advantage of an independent design of dynamic feedforward control and of disturbance reconstruction and compensation. However, the use of integrating process models in SP leads to unobservable and unconstrained output disturbances [30], [31]. Moreover, equivalent output disturbances may increase beyond all limits in the presence of constant input disturbances [32]. Therefore, several authors have tried to avoid the problem of diverging output disturbances by modifying the SP for integrating process models by taking into account the input disturbances [33]–[37]. However, in ensuring internal stability they only succeeded after reducing the overall functionality by eliminating the signal of the reconstructed disturbance. This, finally, severely limited the applicability of the SP control structure.

Only the control structures using the set point and input disturbance reference models [32] can eliminate the hidden internal instability of structures with disturbance observers for unstable plants while maintaining the full functionality of the circuit in terms of disturbance reconstruction. Since the disturbance signal can be critically important in several control, monitoring and diagnostic applications, the development of the reference model control has proven to be important also for systems using time-delayed integrator models.

TABLE 1. List of acronyms and abbreviations.

2DOF	2 Degree of Freedom
ADRC	Active Disturbance Rejection Control
DIPDT	Double Integrator Plus Dead-Time
DOB	Disturbance Observer
DTC	Dead-Time Compensator
ESO	Extended State Observer
FIR	Finite Impulse Response
FOTD	First Order Time Delayed
IAE	Integral Absolute Error
IMC	Internal Model Control
IPDT	Integrator Plus Dead-Time
LADRC	Linear Active Disturbance Rejection Control
MFC	Model-Free Control
M_s, M_t	Maximal Sensitivity, Maximal Complementary Sensitivity
P	Proportional
PD	Proportional-Derivative
PI	Proportional-Integrative
PID	Proportional-Integrative-Derivative
RM	Reference Model
RMC	Reference Model Control
RM-DTC	Reference Model-based Dead-Time Compensator
SDOB	Stabilized Disturbance Observer
SE	Speed-Effort
SOTD	Second-Order Time-Delayed
SP	Smith Predictor
SW	Speed-Wobbling
TV	Total Variation
TV_0	Deviation from monotonicity (0P shape)
TV_1	Deviation from 1P shape
TV_2	Deviation from 2P shape
TOM1A	Arduino-based Thermo-Opto-Mechanical system
QRDP	Quadruple Real Dominant Pole

The novelty of the manuscript thus relates to the overall design of a dead-time compensator for time-delayed chains of first and second order integrators. In particular, the proposed solution allows (1) a decoupled design with (2) decoupled control branches used for separate setpoint tracking and disturbance rejection. The master controller, which ensures the internal stability of the control loop, (3) has a nominal input signal of zero so that it does not affect the transients, and (4) preserves the reconstructed input disturbance signal that can be used for monitoring, diagnostics and optimisation of the control loop. Since the design is based on an ultra-local integrative model, (5) the proposed design can be applied to a wide range of process models that can be approximated by second-order dead-time processes.

To satisfy the requirements to work with disturbance signals even in the case of marginally stable integrator-plus-dead-time (IPDT) and DIPDT models, this work provides a generalization of the control approach with a decoupled setpoint feedforward and disturbance rejection dynamics proposed in [32] for IPDT process models. Thereby, the paper is structured as follows: Section II discusses

two different implementations of setpoint feedforward for second-order systems: the transfer-function-based implementation and the primary-control-loop-based implementation. The requirements for the design of the input disturbance observer based on DIPDT models, as well as the design of the higher-level stabilizing controller and the necessary reference models for setpoint tracking and disturbance rejection are discussed in Section III. Section IV compares the newly designed RM-DTC with PID controllers in terms of achievable performance and robustness. Section V illustrates the developed controller by a real-time example. The results of the simulation verification are summarized in the Conclusions.

II. SETPOINT FEEDFORWARD DESIGN

As commonly applied in motion control [38], the control structure is composed of a feedforward controller and a disturbance observer. These key control structures will be extended by setpoint and disturbance reference models [32] and a stabilizing PD controller [39].

Remark 1 (Basic Loop Modelling Constraints): RM-DTCs have potential to increase the transient quality of high-end applications. As different constraints on the usual plant modelling apply in such situations, such limitations, as the dead-time, nonlinearities, or constraints on the process input and state, need to be given due consideration in the design from the outset.

A. THE SIMPLEST PROCESS MODELLING

The advantage of feedforward over feedback is that any transport delays do not affect the shape of the controlled system transients, but merely delay the time responses. The primary disadvantage of feedforward control is that, without a stabilizing controller, it can only be applied to stable systems. This fundamental limitation can be circumvented by reference model control (RMC). In terms of setpoint tracking, RMC is already part of standard textbooks (see, e.g., [40]). However, its use in disturbance reconstruction and compensation is much less known [32].

From the point of view of modeling more complex and often nonlinear processes, it may be advantageous to use models as simple as possible, such as the DIPDT model. For the process model $F(s)$, which relates the Laplace transform $Y(s)$ of the output $y(t)$ to $U(s)$ of the DIPDT input $u(t)$

$$F(s) = \frac{Y(s)}{U(s)} = \frac{K_s e^{-T_d s}}{s^2} \tag{1}$$

it is necessary to identify only two model parameters K_s and T_d. Thus, the models (1) represent the simplest possible and thereby realistic second-order process approximation. To express differences between the abstraction of the process model $F(s)$ and its estimate used in the controller design, we will introduce the transfer function

$$F_m(s) = \frac{K_m e^{-T_m s}}{s^2} \tag{2}$$

Here K_m represents the estimate of the process gain K_s, which is always unknown. So, by considering $K_s \neq K_m$ when designing the controller, we introduce some uncertainty into the control calculations.

From an identification process that can be carried out in open-loop conditions we get also some estimate of the plant delay T_m. T_m can represent a composition of different loop delays, including the dominant process delay T_p, an actuator dead-time T_a, a communication delay T_c, or a measurement sensor delay T_t, yielding together $T_m = T_p + T_a + T_c + T_t$. In principle, different, or additional delays may occur when implementing closed-loop control. Then, if we still want the controller settings derived for the transfer function (1) to accurately reflect the needs of the real circuit, we usually have to supplement T_m with estimates of the newly introduced delays. These will almost always include the delay of the low-pass filters needed to obtain the feasible controller transfer function. Filter delay can be represented separately by an equivalent dead-time T_e [39]. Then, the total loop delay considered in the design will be calculated as

$$T_d = T_m + T_e \tag{3}$$

Both (1) filtered inversion of the process transfer functions and (2) primary control loops can be used to implement feedforward control. The simulation schemes used to compare both approaches in terms of robustness are shown in Fig. 1. The transfer function of the ''real'' controlled system, which is extended by an unknown internal feedback parameter a, is assumed in the form

$$F(s) = \frac{Y(s)}{U(s)} = \frac{K_s}{s^2 + as} \tag{4}$$

We will use the subscript ''m'' to indicate the parameter estimate of the model used for the control design.

B. PRIMARY-LOOP-BASED FEEDFORWARD CONTROL

For the extended second-order process models (4), the stabilizing controller can always be written as

$$C(s) = \frac{U(s)}{E(s)} = K_P \frac{1 + sT_D}{1 + T_{fd}s} = \frac{K_P + K_D s}{1 + T_{fd}s}, \tag{5}$$

where K_P is the controller gain and T_D is the derivative time constant, which both give the derivative gain K_D. For the implementation of the primary loop with a measurable state shown in Fig. 1, the PD control can ideally be implemented without the derivative filter, i.e., with $T_{fd} = 0$ in (5). For the nominal process model with $a_m = a$; $K_m = K_s$, when from the requirement of a double closed loop time constant T_c one gets

$$K_P = \frac{1}{T_c^2 K_m}; \quad K_D = \frac{2/T_c - a_m}{K_m}; \tag{6}$$

and when there are no input constraints on the process, such feedforward control leads to the closed-loop

transfer functions

$$F_c(s) = \frac{Y(s)}{W(s)} = \frac{1}{(1+T_c s)^2};$$
$$F_{ff}(s) = \frac{U(s)}{W(s)} = \frac{s^2 + a_m s}{K_m(1+T_c s)^2}. \quad (7)$$

As discussed in detail in [32], the advantages of primary-loop-based feedforward control will be evident in unstable systems with input constraints. As shown in Fig. 2 by two simulations with parameters

$$\begin{aligned} T_c &= 0.5; \\ K_s &= 1; \quad K_m = K_s; \\ a &= -0.2; \quad a_m = -0.205; \\ a &= 0.05; \quad a_m = 0; \\ U_{min} &= -0.5; \quad U_{max} = 0.5; \end{aligned} \quad (8)$$

corresponding to parameter uncertainty $\Delta a = a - a_m = 0.05$, the effect of inaccurate parameters is much less pronounced than the effect of constraints, at least in the short run. Surprisingly, the parametric inaccuracy of feedforward has more profound consequences in the simplified position control with a stable speed subsystem $a > 0$. Of course, the uncontrolled feedforward does not guarantee a longer stable setpoint tracking for unstable systems. But when the primary closed-loop feedforward control is used, the results are much better than for the open-loop feedforward control based on transfer function. The differences are mainly to be seen in the course of the output variables.

Remark 2 (Primary DTC Loop Mission): The use of the primary DTC loop (typical for SP) is not related to the transport delay itself, but to the feedforward generation and to the control constraints, which are among the fundamental nonlinearities of the circuit.

As for the effect of the constraints themselves on the shape of the transients of the primary loop, the linear PD controller can handle smaller constraints without disturbing the smooth shapes of the transients. For more significant constraints, a constrained design must already be used (see, e.g., [5], [41]–[43]).

C. SETPOINT REFERENCE MODEL

It is well known that open-loop feedforward control cannot be used to control unstable and marginally stable processes. In combination with a higher-level stabilization controller and a reference model, the advantages of feedforward control (e.g., in terms of time-delayed process control) can be exploited [32], [40]. The reference model ensures the hierarchical division of activity between the stabilizing controller and feedforward control by providing the higher-level controller with information about the correct course of the setpoint tracking initiated by the feedforward control. For example, for the closed-loop (setpoint to process output) transfer function $F_c(s)$ (7), the control error, defined as

$$E_w(s) = F_c(s)W(s) - Y(s) \quad (9)$$

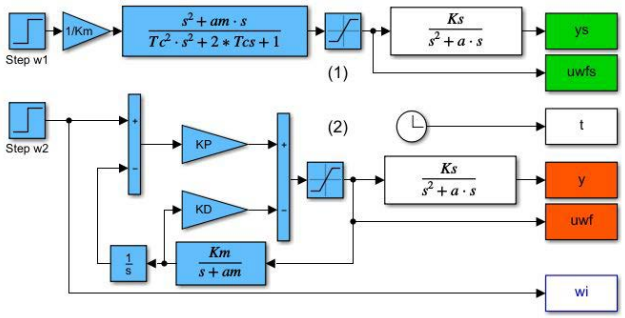

FIGURE 1. 1. Open loop (transfer function-based) and 2. primary-loop (PD control-based) constrained setpoint feedforward implementations for setpoint steps of w with parameters (6) used to explain advantages of closed-loop-based feedforward implementation.

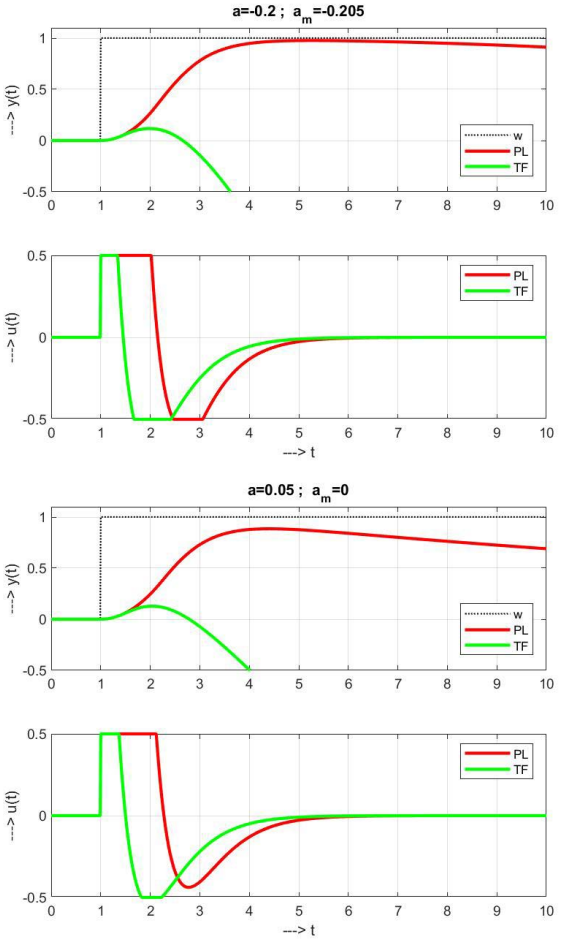

FIGURE 2. Process input and output in transfer function-based (TF) and primary-loop-based (PL) constrained setpoint feedforward for unit setpoint steps of w according to Fig. 1 and $a = -0.2$, $a_m = -0.205$ (above) and $a = 0.05$, $a_m = 0$ (below) showing advantages of the closed-loop-based feedforward implementation; $K_m = K_s = 1$, $T_c = 0.5$, $U_{max} = 0.5$, $U_{min} = -0.5$.

will be nominally zero. The processing of the control error by the PD controller (5)-(6) (with $a_m = 0$) does not cause any effect, but ensures the stability of the closed loop even in unstable systems. For primary control, the signal $F_c(s)W(s)$ can be taken directly from the output of the plant model

output. For a delay-free plant, such a controller could be proposed by omitting all the transport delay blocks T_m and T_d in Fig. 3 (e.g., by setting $T_d = T_m = T_{m1} = T_{m2} = 0$). However, later we will also deal with the time-delayed systems, while also focusing on the reconstruction and compensation of disturbances.

III. DISTURBANCE RECONSTRUCTION AND FEEDFORWARD

The basic idea of the input disturbance observer is to evaluate the difference between the process input estimated from the output using the inverse process model and the controller output. Low-pass filters with sufficiently high relative degree must also be introduced to perform the given operation. The presence of a transport delay (as in Fig. 3) naturally complicates the whole control process, since there is no inversion to the delay in causal systems and its influence must be mitigated in other ways. The first DTCs for DIPDT processes reduced the loop delay by reconstructing less delayed outputs and disturbance signals [10]. Such an approach was no longer a violation of causality, but a replacement of the transport delay by the delays of the observer filters. In turn, such solutions increased the speed of the transients and improved disturbance rejection performance. Works [33], [44] based on independent setpoint and disturbance feedforward loops without a stabilizing controller encountered the problems with internal instability in unstable and marginally stable systems, which they could solve only by eliminating the disturbance signal from the control structure. The mentioned works did not respect the fundamental property of disturbance observers [32], [45], which is not only reconstructing disturbance, but at the same time, the controlled object is forced to follow the nominal dynamics of the chosen model. Thereby, in terms of external disturbance reconstruction, the nominal model must be chosen as close as possible to the controlled process. However, the unstable nominal model does not then guarantee the stability of the solution in the long run. The conflicting requirements on precise plant modelling with respect to disturbance reconstruction and compensation and internal stability have been solved just by introducing stabilizing controller and disturbance reference models [32]. In RM-DTCs, the higher-level stabilization controller ensures the stability of the overall loop, but does not interfere with the nominal transients specified at the slave level with setpoint and disturbance feedforward loops. For better clarity, we divide the overall disturbance feedforward design into two steps, the first describing the observer design with a reference model for a system with negligible dead time and just then including also the dead-time term.

A. DISTURBANCE REFERENCE MODEL FOR DELAY-FREE MODEL

To make the inverse of the process model (2) feasible, the disturbance observer must use the low-pass filter $Q_i(s)$:

$$Q_i(s) = \frac{1}{(1+T_o s)^2}. \tag{10}$$

For an independent application of disturbance reconstruction and compensation, the disturbance response must be stable. Two unstable plant poles can be eliminated from the disturbance response by the disturbance feedforward

$$C_i(s) = \frac{1 + b_1 s + b_2 s^2}{(1+T_o s)^{n-2}}; \quad n \geq 4, \tag{11}$$

with n denoting the total filter order. With the lowest possible value $n = 4$ and designation

$$S_{uu}(s) = C_i(s) Q_i(s) \tag{12}$$

and considering the reconstruction of the actual plant input $U_{af}(s)$

$$S_{yu}(s) = \frac{U_{af}(s)}{Y(s)} = \frac{S_{uu}(s)}{F_m(s)} = \frac{s^2(1 + b_1 s + b_2 s^2)}{K_m (T_o s + 1)^4}, \tag{13}$$

the disturbance compensation signal can be calculated as

$$U_{if}(s) = S_{yu}(s) Y(s) - S_{uu}(s) U(s). \tag{14}$$

In the nominal case with $K_s = K_m$ and $F(s) = K_s/s^2 = F_m(s)$, we get a "stabilized" disturbance response

$$F_{iy}(s) = \frac{Y(s)}{D_i(s)} = \frac{F}{1 + F_u S_{yd} F}; \quad F_u = \frac{1}{1 - S_{uu}}. \tag{15}$$

Note that to cancel the double plant pole $s = 0$ and to get the zero steady-state disturbance response characterized with $F_{iy}(0) = 0$, the numerator in

$$F_{iy}(s) = K_s \frac{(1+T_o s)^4 - (1 + b_1 s + b_2 s^2)}{s^2 (1+T_o s)^4} \tag{16}$$

has to guarantee the triple pole at $s = 0$. Let us use the new variable $p = T_o s$, $\beta_1 = b_1/T_o$, $\beta_2 = b_2/T_o^2$, to simplify the calculation. Then

$$F_{iy}(p) = K_s T_o^2 \frac{(1+p)^4 - (1 + \beta_1 p + \beta_2 p^2)}{p^2 (1+p)^4}. \tag{17}$$

By comparing the coefficients at the first and second power of p we get the required values β_1, β_2 and subsequently also b_1, b_2, which yields

$$\begin{aligned} \beta_1 &= 4; \quad \beta_2 = 6; \ \alpha_0 = 4; \\ F_{iyo}(p) &= K_s T_o^2 \frac{p(p+\alpha_0)}{(1+p)^4}. \end{aligned} \tag{18}$$

In the "s" domain with the same value of $\alpha_0 = 4$,

$$\begin{aligned} b_1 &= 4T_o; \quad b_2 = 6T_o^2; \\ F_{iyo}(s) &= \frac{Y(s)}{D_i(s)} = K_s T_o^3 \frac{s(T_o s + \alpha_0)}{(1+T_o s)^4}. \end{aligned} \tag{19}$$

At this point, however, it should be emphasized that a stabilized disturbance response does not imply a stabilized system state. Through reconstruction and disturbance compensation, the system behaves according to the chosen model $F_m(s)$, i.e., as a marginally stable double integrator with gain K_m. To obtain a system with stabilized states, an additional stabilizing controller is required. Such a controller can be designed according to expressions (5)-(6) with $a_m = 0$,

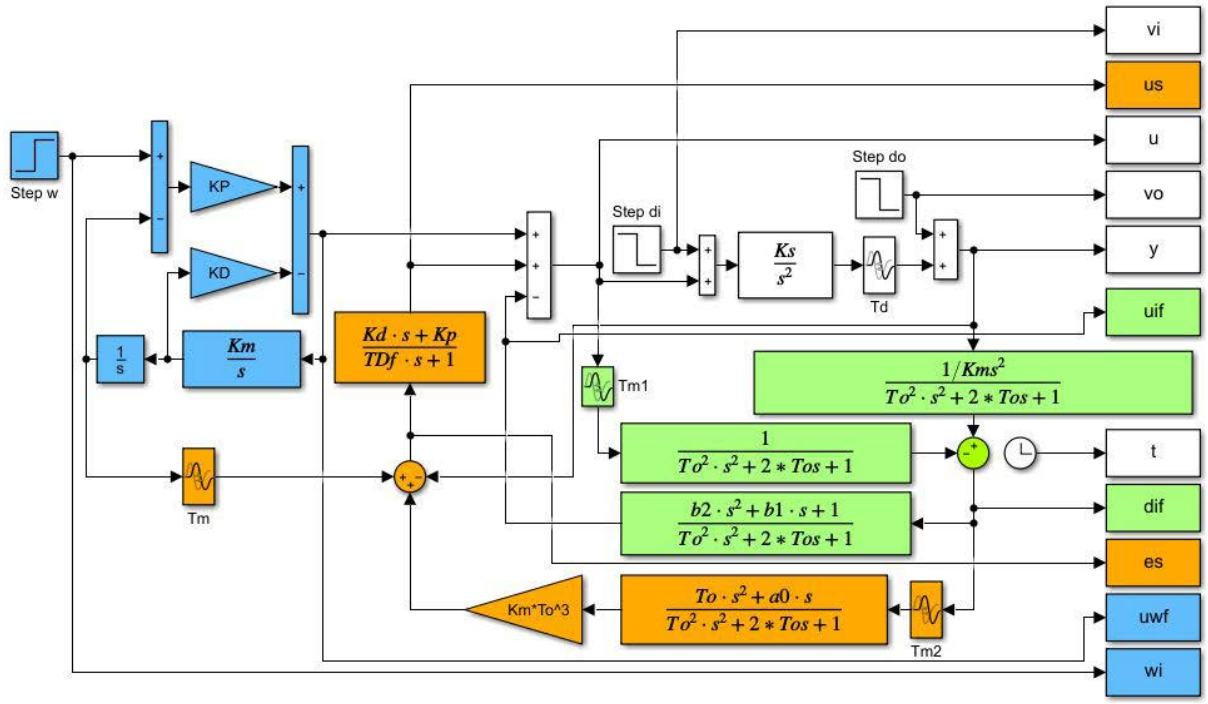

FIGURE 3. Setpoint feedforward (blue), SDOB-based disturbance feedforward (green) and stabilizing PD controller $K_P + K_d s$ with reference model $Q_w(s) = F_{wy}(s)$ from the setpoint w and $F_i(s) = F_{iy}(s)$ from the reconstructed disturbance d_i (orange) as the basic units of the RMC for the DIPDT system with model (2).

where a suitable derivative filter time constant T_{fd} should be chosen. Since the nominal disturbance response is given by the transfer function $F_{iyo}(s)$ (18) and the DOB gives the disturbance signal filtered by the second-order $Q_i(s)$, the wanted disturbance reference model RMi is

$$F_i(s) = \frac{F_{iyo}(s)}{Q_i(s)} = K_s T_o^3 \frac{s(T_o s + \alpha_0)}{(1 + T_o s)^2}. \tag{20}$$

The examples of the setpoint and disturbance step responses obtained by the controller scheme in Fig. 3 for $T_d = T_m = 0$ and the parameters

$$\begin{aligned} &T_c = T_o = 0.8; \quad K_s = 1; \; K_m \in \{0.8, 1, 1.2\}; \\ &K_p = K_P; \quad K_d = K_D; \; T_{fd} = 0.2 \end{aligned} \tag{21}$$

are presented in Fig. 4. The choice of these parameters was motivated by the possibility to compare the obtained transients with the further analysed loop with dead time. They show that the plant gain perturbation produced by $K_m \neq K_s$ corresponds to an input disturbance that increases as T_c and T_o decrease.

Remark 3 (The Main Advantage of RM-DTCs): Besides the generalization shown for the double integrator, the main advantage of the newly introduced reference model control over the solutions in [33]–[37] is the availability of the equivalent input disturbance signal, which can be of great use for finding the optimal process model and for its further diagnosis. From the opposite signs of the reconstructed disturbance signal (d_{if}) in the initial interval without external disturbances for the non-nominal values $K_m = 0.8$ and $K_m = 1.2$ in Fig. 4, it is evident that the actual value of the process gain $K_m = 1$ should lie between these two values. Thus, the advantage of keeping the full functionality of the RM-DTC is that it allows monitoring and diagnostics of the controlled process [46], [47].

B. REFERENCE MODEL FOR TIME-DELAYED SYSTEM

The obtained solution can be further extended with nonzero dead time values. From the point of view of setpoint tracking, the extension can be easily achieved by including the dead time model T_m in the reference model of setpoint signal tracking (Fig. 3). While the feedforward transfer function remains the same as in (7), the reference-to-output transfer function $F_c(s)$ corresponding to a double real-time constant T_c becomes

$$F_c(s) = \frac{Y(s)}{W(s)} = \frac{e^{-T_d s}}{(1 + T_c s)^2}. \tag{22}$$

To equate both the process delay T_d and the DOB delay, the time delay T_{m1} must be included in the DOB path from the controller output. In the nominal case with $T_{m1} = T_d$, $S_{uu}(s)$ (12) is changing to

$$S_{uu}(s) = C_i(s) Q_i(s) e^{-T_d s}. \tag{23}$$

For $p = T_o s$, $\tau_d = T_d / T_o$, the disturbance response becomes

$$F_{iy}(p) = K_s T_o^2 e^{-\tau_d p} \frac{(1+p)^4 - (1 + \beta_1 p + \beta_2 p^2) e^{-\tau_d p}}{p^2 (1+p)^4}. \tag{24}$$

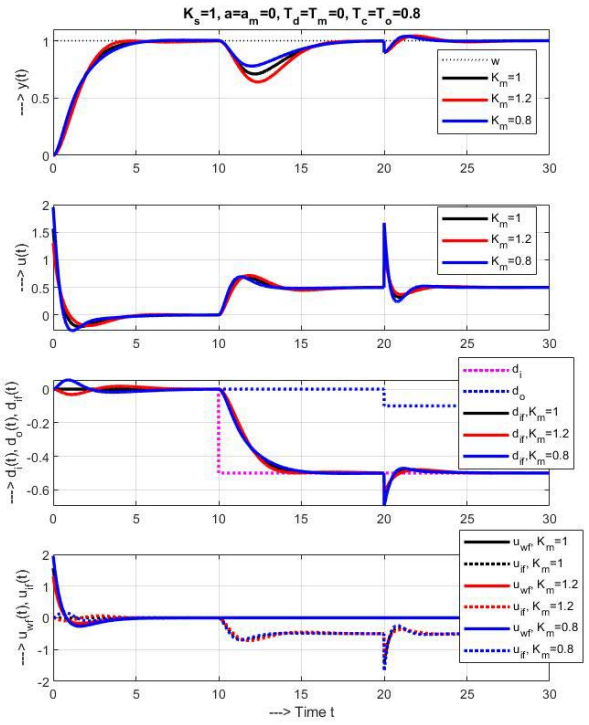

FIGURE 4. Transients with RM-DTC and $T_d = T_m = 0$ showing for different K_m impact of the plant model gain uncertainty, $K_s = 1$; d_i step at $t = 10$, d_o step at $t = 20$; $T_c = T_o = 0.8$.

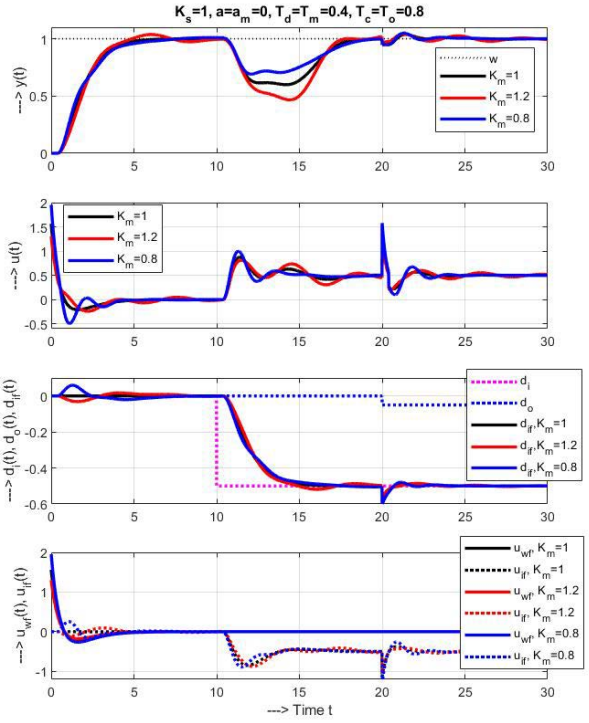

FIGURE 5. Transients with RM-DTC and $T_d = T_m = 0.4$ showing for different K_m impact of the plant model gain uncertainty in the case of time-delayed systems, $K_s = 1$; d_i step at $t = 10$, d_o step at $t = 20$; $T_c = T_o = 0.8$.

A direct comparison of expressions (24) and (17) is not possible because of the time delay. However, in (17), the parameter α_0 could also be obtained by triple derivation of the $F_{iyo}(p)$ numerator $K_s T_0^2 p^3(p+\alpha_0)$, by substituting $p = 0$ and dividing by 3!=6. Similarly, by evolving the numerator of expression (24) we get

$$\alpha_0 = 4 + 6\tau_d + 2\tau_d^2 + \tau_d^3/6\,. \tag{25}$$

For $T_{m2} = T_d$ in Fig. 3, (24) and (18) become equivalent when

$$b_1 = 4T_o + T_d; \quad b_2 = 6T_o^2 + 4T_oT_d + T_d^2/2;$$
$$F_{iyo}(s) = K_s T_o^3 e^{-T_d s}\frac{s(T_o s + \alpha_0)}{(1+T_o s)^4}. \tag{26}$$

From $F_{iyo}(s)$ it is then possible to calculate $F_i(s)$ according to (20).

Design of a stabilizing PD controller for the DIPDT plant model based on the multiple real dominant pole [6], [48], [49], results in parameters

$$K_p = 0.079/(K_s T_d^2); \quad K_d = 0.461/(K_s T_d)\,. \tag{27}$$

The low-pass filter with time constant T_{fd}, which is necessary to realize a stabilizing PD controller of the form (5) has no major influence in the considered controller structure. In Fig. 5, transients corresponding to the parameters

$$a = a_m = 0; \quad T_d = T_m = 0.4;\ T_c = T_o = 0.8;$$
$$K_s = 1; \quad K_m \in \{0.8, 1, 1.2\};\ T_{fd} = T_m/2 = 0.2, \tag{28}$$

with K_P, K_D (6) and K_p, K_d (27), have similar shapes as for $T_d = 0$. Again, note that the choice of T_c and T_o values is taken into account to show the differences that arise due to the influence of T_d and in relation to the model uncertainty considered. In the illustrative example, we will show their significance in terms of taking into account the measurement noise. However, d_i is now reconstructed with a time delay T_m, so the effect on the disturbance response is much stronger. Again, in the case of non-nominal setpoint changes with $K_m \neq K_s$, the equivalent disturbances can already be observed during the periods without external disturbances.

IV. COMPARISON WITH 2DOF PID CONTROL

Comparing the proposed solution with alternative methods based on a PID controller is not straightforward. For example, Grimholt and Skogestad [9] choose the tradeoff between servo and regulatory by optimizing a weighted average of the integral of the absolute error

$$IAE = \int_0^\infty |e(t)|\,dt; \quad e = w - y, \tag{29}$$

during process input and output disturbance steps, but they do not consider the design of a setpoint prefilter to ensure monotonic tracking of the reference steps. The aforementioned solution also does not deal with a suitable controller low-pass filter design that would result in a feasible, fully implementable transfer function of the controller to attenuate

a measurement noise and to minimize the excessive signal increments at the plant input.

At the plant output, a modification of the total output variation criterion (TV) [50]

$$TV_0(y_s) = \sum_i (|y_{i+1} - y_i|) - |y_\infty - y_0| \tag{30}$$

can be interpreted as the output's deviation from monotonicity. At the plant input, the excessive control effort can be defined in terms of the deviations from the two-pulse (2P) control signal. For the double integrator, the expected control signal consists of the two extremes u_{m1} and u_{m2}, which lie at some time instants between the initial value u_0 and the final u_∞ of the control signal and have the amplitudes $u_{mi} \notin [u_0, u_\infty]; i = 1, 2;\ (u_{m1} - u_\infty)(u_{m2} - u_\infty) < 0$. Ideally, such a signal has three monotonic intervals [39], [51], [52]. The plant input deviation from 2P shape can be calculated as follows

$$TV_2(u) = \sum_i (|u_{i+1} - u_i|) - |2u_{m1} - 2u_{m2} + (u_\infty - u_0)\,\mathrm{sign}(u_{m1} - u_\infty)|\,. \tag{31}$$

Remark 4 (Reason for Changed Evaluation Excessive Control Effort): In contrast to the definition of TV given in [50], the application of (31) does not penalize active changes in the controller output forced by the necessary acceleration and deceleration of the process. Such shortcomings in the evaluation of the control effort are encountered in the majority of recent publications and the separation of useful control actions from redundant ones is only slowly being promoted [23], [53], [54].

A. THE MULTIPLE REAL DOMINANT POLE PID CONTROLLER TUNING

Unlike [55], which is dominantly dealing with control constraints, without considering the transport delays and noise attenuation, the limitations are only briefly mentioned here, without a detailed evaluation. The considered analytically derived optimal PID controller is based on a generalization of the approach used in [56], [57].

As shown in Theorem 1 in [39], for the parameters $T_d > 0, K_s \neq 0$ of model (1), for ideal PID controller with parameters K_c (the controller gain), T_i (the integral time constant) and T_D (the derivative time constant)

$$C(s) = \frac{U(s)}{E(s)} = K_c\left(1 + \frac{1}{sT_i} + sT_D\right) \tag{32}$$

the "optimal" values K_{co}, T_{io} and T_{Do} can be determined analytically to ensure a quadruple real dominant pole (QRDP) s_o of the characteristic quasi-polynomial

$$P(s) = T_i s^3 e^{T_d s} + K_c K_s(1 + T_i s + T_i T_D s^2) \tag{33}$$

such that

$$s_o = -0.416/T_d. \tag{34}$$

These values may be expressed by dimensionless (normalized) parameters κ_o, τ_{io} and τ_{Do} as

$$\begin{aligned} \kappa_o &= K_{co}K_s T_d^2 = 0.125, \\ \tau_{io} &= T_{io}/T_d = 10.324, \\ \tau_{Do} &= T_{Do}/T_d = 4.043. \end{aligned} \tag{35}$$

For zero compensation of the closed loop transfer function

$$F_{w0}(s) = \frac{Y(s)}{W(s)} = \frac{K_c K_s(1 + T_i s + T_i T_D s^2)}{T_i s^3 e^{T_d s} + K_c K_s(1 + T_i s + T_i T_D s^2)} \tag{36}$$

leading to overshoot after reference setpoint steps, [56], [57] proposed the two-degree-of-freedom (2DOF) PID using a setpoint prefilter [51]

$$F_p(s) = \frac{cT_i T_D s^2 + bT_i s + 1}{T_i T_D s^2 + T_i s + 1}\,. \tag{37}$$

In the simplest case, $F_p(s)$ is used with

$$b_0 = c_0 = 0\,. \tag{38}$$

To accelerate the transients, the weighting parameters b and c can also be set to cancel one of the quadruple closed loop poles s_o (34)

$$b_1 = \frac{1/|s_o|}{T_{io}} = -\frac{1}{\tau_{io}T_d s_o} = 0.233 \quad c_1 = 0. \tag{39}$$

The fastest possible setpoint step responses correspond to the numerator of (37), which is equal to the double pole s_o:

$$(s - s_o)^2 = s^2 - 2ss_o + s_o^2 = s^2 + bs/(cT_D) + 1/(cT_iT_D). \tag{40}$$

This gives the prefilter coefficients

$$b_2 = -2/(T_i s_o) = 0.466, \quad c_2 = 1/(T_i T_D s_o^2) = 0.150. \tag{41}$$

However, such a design increases the required control signal amplitudes (see Fig. 6) and also the overshoot due to gain uncertainty.

Finally, to obtain a feasible controller transfer function, $C(s)$ must be combined with a first-order series filter [51]

$$Q\,(s) = 1/(T_1 s + 1) \tag{42}$$

with the time constant $T_1 = 0.271T_e$ expressed by means of an equivalent dead-time T_e. It has been considered in the controller tuning as an additional delay $T_e = 0.4$, added to the total dead time of the control loop.

Since it is generally difficult to obtain good performance for a double integrating process, when the time delay T_d is large, cascade control is used in practice whenever possible for controlling double integrating processes [9], [51].

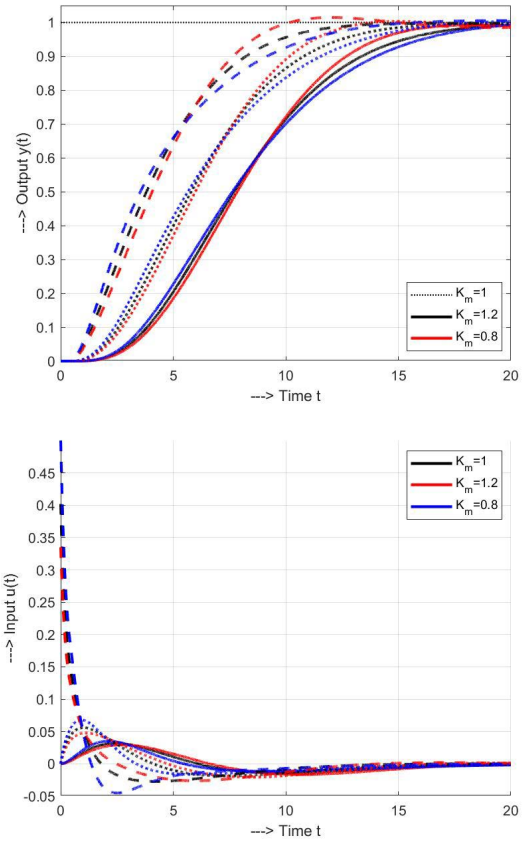

FIGURE 6. Setpoint step responses of the PID controller (32) with the tuning (35), filter (42) and prefilter (37)showing for different K_m impact of the plant model gain uncertainty.

B. ROBUSTNESS TESTS BY NEW PERFORMANCE SENSITIVITY MEASURES

Traditional robustness analysis is mostly based on sensitivity functions [58], which are defined for the open-loop transfer function $L(s)$ as

$$M_s = \max\left\{\left|\frac{1}{1+L(j\omega)}\right|\right\}; \quad M_t = \max\left\{\left|\frac{L(j\omega}{1+L(j\omega)}\right|\right\}; \quad \omega \geq 0. \tag{43}$$

M_s is primarily defined for the nominal loop and is related to the loop stability. The recommended values of the sensitivity function are usually less than 2 and are generally not suitable for unstable systems, where the required sensitivity values may increase to more than 20 [59]. Therefore, instead of using sensitivity functions, we preferred to implement the robustness test similar to the approach proposed in [60]. In such a test, the controller based on model (2) is applied to the plant (4) extended by a dead time

$$S(s) = \frac{Y(s)}{U(s)} = \frac{e^{-0.4s}}{s(s+a)}; \quad a \in [-0.2, 0.2]; \ \Delta a = 0.1. \tag{44}$$

Its internal feedback, quantified by the pole $s = -a$, transforms the DIPDT plant into the second-order time-delayed system (SOTD) (44). By changing a in (44), the performance measures corresponding to the setpoint steps under DIPDT-based controller draw trajectories in the speed-effort (SE) plane ($IAE - TV_2(u)$) and speed-wobbling (SW) plane ($IAE - TV_0(y)$), as shown in Fig. 7. Here, longer trajectories correspond to stronger performance changes and hence higher sensitivity (lower robustness) of the control loop. Denote the individual uncertain parameter values as

$$a_i = a_{min} + (i-1)\Delta a; \quad i = 1, 2, \ldots, N; \\ \Delta a = (a_{max} - a_{min})/(N-1), \tag{45}$$

and the coordinates of the performance measures vector (ξ, η) as

$$\xi = TV_2(u), \text{ or } \xi = TV_0(y); \quad \eta = IAE. \tag{46}$$

The corresponding sensitivity measures for the setpoint responses at the plant input, or output, reflecting the length of the trajectory traced out by the change in position of the operating point (46), can then be defined as

$$S = \sum_{i=1}^{N-1} \sqrt{(\xi_i - \xi_{i+1})^2 + (\eta_i - \eta_{i+1})^2}. \tag{47}$$

The introduction of these new sensitivity measures $S(u)$ and $S(y)$, in contrast to the traditional M_s and M_t sensitivity peaks, brings the differentiation of the achieved sensitivity levels with respect to the input and output of the system, as well as the consideration of the controller effort required to maintain the required performance at the input or output.

The results in Fig. 7 were evaluated taking into account the measurement noise with a maximum amplitude of 0.001 generated in Matlab-Simulink by the Uniform Random Number block. Corresponding to PID control with different prefilters (38)-(41) they show that by using more complex prefilters we can speed up the transients while keeping nearly the same excessive control effort (Fig. 7 left). However, at the cost of larger output fluctuations in performance when changing the internal system feedback parameter a (Fig. 7 right). For RM-DTC, the results vary to a greater extent. The smallest value of the tuning parameter $T_c = T_o = T_d/2$ leads to the fastest transients (minimal IAE) with the lowest dependence on the perturbed parameter (reflected by low $S(u)$ and $S(y)$ values). However, this is achieved on the costs of the highest excessive controller effort $TV_2(u)$, reminiscent of robust systems using sliding mode control [61], [62].

The $TV_2(u)$ values can be reduced to by increasing T_c and T_o. In general, we achieve optimal values of $S(u)$, $S(y)$ and $S(u)S(y)$ (see Fig. 8) with different settings, which challenges the design according to M_s and M_t criteria.

Of course, the impact of measurement noise can also be reduced by using higher order filters in DOB, or in the stabilizing controller.

Remark 5 (Impact of the Feedback Parameter a, ADRC, PID and DTC Design): The characteristics in Fig. 7 also show that the influence of the parameter a on the excessive controller effort and the speed of transients is negligible

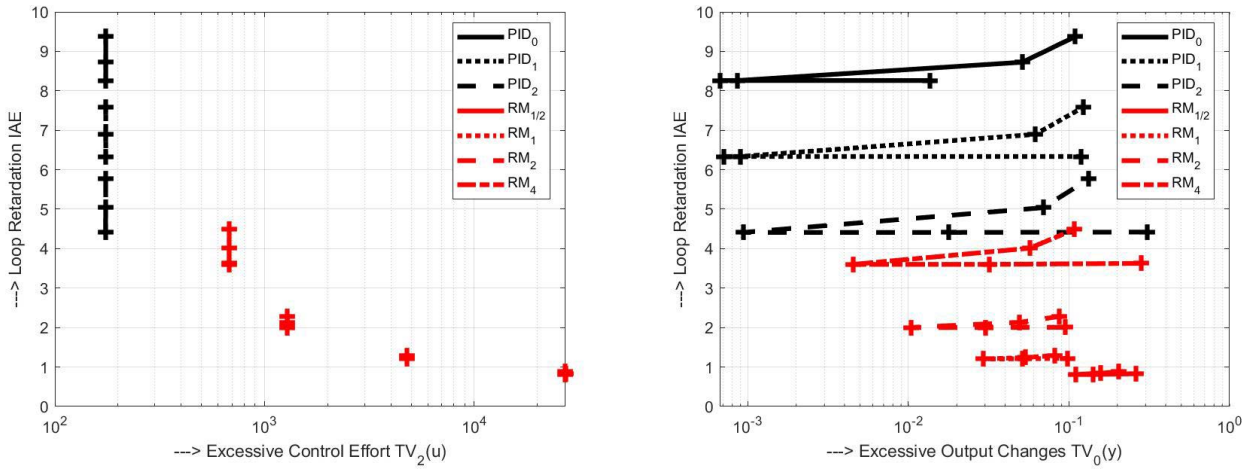

FIGURE 7. Robustness characteristics expressing *IAE* changes due to uncertainty of the internal plant feedback coefficient a versus the shape related deviations at the input of the plant (44), $\Delta a = 0.1$ and different PID controllers tuned with $T_e = T_d = 0.4$ and prefilters (38)-(41) and the RM-DTCs with the parameters $T_c = T_o \in \{1/2, 1, 2, 4\}T_d$; $K_m = K_s = 1$; measurement noise amplitude $|\delta| \leq 0.001$.

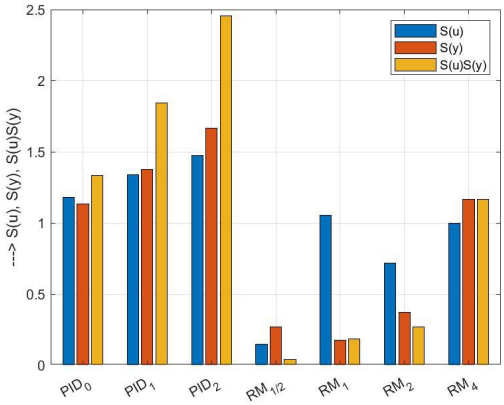

FIGURE 8. Sensitivities (46)-(47) defined for the plant (44) with uncertain a and *PID* controllers tuned with $T_e = T_d = 0.4$ and prefilters (38)-(41) and the RM-DTCs with the parameters $T_f = T_o \in \{1/2, 1, 2, 4\}T_d$; $K_m = K_s = 1$.

compared to the effect of the measurement noise. This makes it possible to avoid identification of this parameter and so to simplify the controller design. Similar feature represents one of the key reasons for the popularity of ADRC. However, such simplification is clearly also relevant in designing RM-DTCs and can also be shown in PI and PID control [63].

V. ILLUSTRATIVE EXAMPLE: TEMPERATURE CONTROL

The decoupled setpoint tracking and disturbance rejection, together with the use of a superior stabilizing controllers, have created new degrees of freedom in tuning of RM-DTCs compared to traditional PID controllers. Therefore, it will be useful to start clarifying the increased tuning complexity by explaining particular tuning steps, preferably from the simplest tasks. To illustrate the use of the RM-DTC design and practical problems associated with its application, we will consider the thermal process control discussed already in [31], [60], [64]. The choice of this process is motivated by several aspects - from a physical point of view, it is a highly nonlinear and time-variable higher-order process posing a challenge for robust control - only due to the fact that the concept of a nominal dynamics is strongly questionable. The existing time delays and the resulting measurement noises also require due attention to the appropriate filtering of the measured signals. In addition, it is a process that is clearly not integrative. So, the use of integrative models is not a meaningful step for many users and needs to be shown that it can still be beneficial. Nevertheless, it makes it possible to clarify several aspects of RM-DTC control based on IPDT models and subsequently to highlight the specifics of control of systems with DIPDT models.

A. SIMPLIFIED PLANT MODELLING

The essence of thermal process control is to vary the amount of heat released by the actuator (bulb) so that the temperature measured at the desired point (by a sensor *pt*1000) reaches in the shortest time possible the setpoint reference value. Among the different possible ways of heat transfer participating in heating the temperature sensor (such as advection, conduction convection, radiation, boiling, condensation, or melting), occur in the case of the thermo-optical-mechanical laboratory system TOM1A [65] mainly the fastest heat transfer by radiation and conduction. So, although a physically more accurate modeling of the dynamics of the system under consideration would require the use of higher-order models, limiting to the fastest process mode it is usually enough to work with the IPDT model

$$F(s) = \frac{Y(s)}{U(s)} = \frac{K_s}{s} e n^{-T_d s}. \tag{48}$$

Parameters of the plant model identified in the vicinity of the selected operating point and applied in works [31], [64] can be given as

$$K_s = 0.01; \quad T_d = 0.3\text{s}. \tag{49}$$

The identified internal feeddback coefficient $a = 0.05\text{s}^{-1}$, corresponding to a time constant $T = 1/a = 20\text{s}$, will be neglected. (From this moment on, we stop emphasizing that these are the parameters of the model and we simply write K_s and T_d instead of K_m and T_m.)

B. IPDT-BASED RM-DTCs

Firstly, since the RM-DTC designed in [32] with a second-order low-pass filter (used in the disturbance observer and the disturbance feedforward) proved to be insufficient for a noisy environment, its extension had to be developed to more effectively reduce noise. To illustrate the practical aspects of such a design continuing from simpler to more complex setup, let us first consider controller design based on a first-order integral model (i.e., $T_d = 0$)

$$F(s) = \frac{Y(s)}{U(s)} = \frac{K_s}{s}. \tag{50}$$

In this case, use just the P controller

$$u_w = K_P(w - y); \quad K_P = 1/(T_c K_s) \tag{51}$$

to generate the setpoint feedforward control. For the disturbance feedforward the parameters b^n corresponding to the total filter degree n with

$$Q_1(s) = \frac{1}{1 + T_o s}; \quad C_i(s) = \frac{1 + b^n s}{(1 + T_o s)^{n-1}}; \; n \geq 2, \tag{52}$$

the disturbance compensation signal can be calculated as

$$\begin{aligned} U_{if}(s) &= S_{yu}(s)Y(s) - S_{uu}(s)U(s); \\ S_{yu}(s) &= \frac{U_{af}(s)}{Y(s)} = \frac{s(1 + b^n s)}{K_s(T_o s + 1)^n}; \\ S_{uu}(s) &= \frac{1 + b^n s}{(T_o s + 1)^n}. \end{aligned} \tag{53}$$

From (53) we get the "stabilized" disturbance response

$$\begin{aligned} F_u &= \frac{1}{1 - S_{uu}}; \\ F_{iy}^n(s) &= \frac{F}{1 + F_u S_{yu} F} = K_s \frac{(T_o s + 1)^n - (1 + b^n s)}{s(T_o s + 1)^n}. \end{aligned} \tag{54}$$

To simplify the calculation of a stable F_{iy}^n, let us again use the variable $p = T_o s$ and parameters $\beta^n = b^n/T_o, \kappa = K_s T_o$, when

$$F_{iy}^n(p) = \kappa \frac{(p + 1)^n - (1 + \beta^n p)}{p(p + 1)^n} \tag{55}$$

Since an elimination of the numerator coefficient at p yields

$$\beta^n = n; \quad b^n = nT_o \tag{56}$$

and due to this choice the lowest two numerator coefficients in $F_{iy}^n(p)$ disappear,

$$F_{iyo}^n(p) = \kappa \frac{\sum_{j=2}^{n} \binom{n}{j} p^{j-1}}{(p + 1)^n}. \tag{57}$$

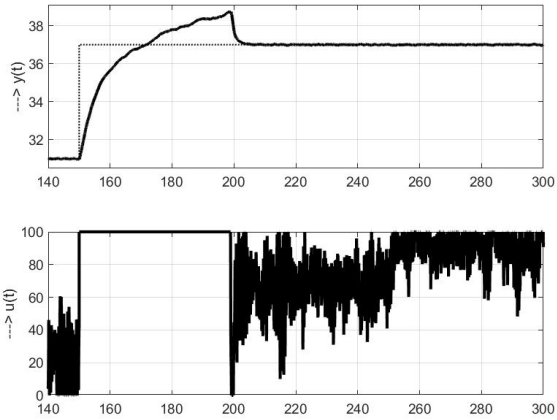

FIGURE 9. Reference model control in Matlab/Simulink based on IPDT model with saturation nonlinearity at the controller output applied to the thermal channel of TOM1A system for the setpoint change from $w = 31$ to $w = 37^oC$ at $t = 150$s and for the fan voltage step from $d_i = 5$ to $d_i = 15$ at $t = 250$s; $T_o = T_d = 0.3$s; $n = 2$; $K_s = 0.01$; $K_p = K_P$ (65).

Therefore, by increasing n we get gradually transfer functions

$$\begin{aligned} F_{iyo}^2(p) &= \kappa p \frac{1}{(p + 1)^2}; \\ F_{iyo}^3(p) &= \kappa p \frac{p + 3}{(p + 1)^3}; \\ F_{iyo}^4(p) &= \kappa p \frac{p^2 + 4p + 6}{(p + 1)^4}; \end{aligned} \tag{58}$$

corresponding to

$$\begin{aligned} F_{iyo}^2(s) &= K_s T_o^2 s \frac{1}{(T_o s + 1)^2}; \\ F_{iyo}^3(s) &= K_s T_o^2 s \frac{T_o s + 3}{(T_o s + 1)^3}; \\ F_{iyo}^4(s) &= K_s T_o^2 s \frac{T_o^2 s^2 + 4T_o s + 6}{(T_o s + 1)^4}; \end{aligned} \tag{59}$$

Instead of calculating the $F_{iyo}^n(p)$ numerator by comparing the coefficients at individual powers of p, the tuning β^n and coefficients α_j^n could also be evaluated to get zero values of the numerator (55) derivatives according to p at $p = 0$, when from

$$\begin{aligned} N_0^n(p) &= (p + 1)^n - (1 + \beta^n p) \\ &= 1 + \alpha_1^n p + \alpha_2^n p^2 + \alpha_3^n p^3 \ldots + \alpha_n^n p^n - (1 + \beta^n p), \\ N_j^n(p) &= \frac{dN_{j-1}^n(p)}{dp}; \quad j = 1, 2, \ldots, n, \end{aligned} \tag{60}$$

follows

$$\beta^n = N_1^n(0); \quad \alpha_j^n = \frac{N_j^n(0)}{j(j-1)\ldots 1}; \; j = 2, 3, \ldots, n. \tag{61}$$

The calculation according to (61) is preferred in the case of time-delayed integrator, when the numerator of $F_{iy}^n(p)$ is

$$N_0^n(p) = (p + 1)^n - (1 + \beta^n p)e^{-\tau_d p}. \tag{62}$$

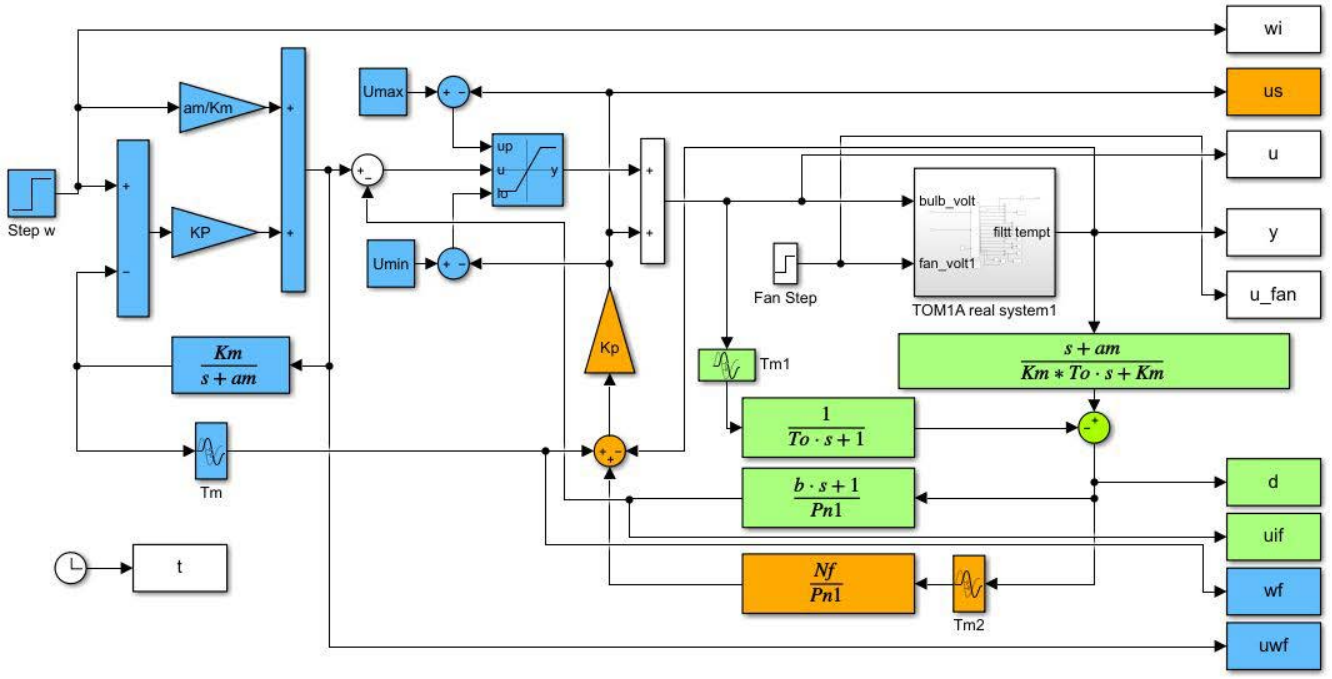

FIGURE 10. IPDT: Reference model control scheme for the thermo-opto-mechanical systems TOM1A proposed by modification of the scheme in Figure 12 in [32], by considering higher order noise attenuation filters in the disturbance feedforward (52) and in the disturbance response $F^n_{iyo}(s)$ (63) applied in Matlab/Simulink with $K_m = K_s$, $T_m = T_d$, $a_m = 0$ (49); $F_i(s) = N_f(s)/P_{n1}(s)$; $P_{n1}(s) = (1 + T_o s)^{n-1}$.

With the help of computer algebra system we can then easily get

$$b^n = nT_f + T_d; \quad F^n_{iyo}(s) = K_s s \frac{N_{iy}(s)}{(T_o s + 1)^n}, \tag{63}$$

where

$$\begin{aligned}
n &= 2;\\
N^2_{iy}(s) &= T_o^2 + 2T_oT_d + T_d^2/2;\\
n &= 3;\\
N^3_{iy}(s) &= A_{31}s + A_{30};\\
A_{31} &= T_o^3 - 3T_o^2T_d - \frac{9}{2}T_oT_d^2 - \frac{5}{6}T_d^3;\\
A_{30} &= 3T_o^2 + 3T_oT_d + T_d^2/2;\\
n &= 4;\\
N^4_{iy}(s) &= A_{42}s^2 + A_{41}s + A_{40};\\
A_{42} &= T_o^4 - 4T_o^3T_d + 3T_o^2T_d^2 + \frac{14}{3}T_oT_d^3 + \frac{17}{24}T_d^4;\\
A_{41} &= 4T_o^3 - 6T_o^2T_d - 6T_oT_d^2 - \frac{5}{6}T_d^3;\\
A_{40} &= 6T_o^2 + 4T_oT_d + T_d^2/2;\\
n &= 5;\\
N^5_{iy}(s) &= A_{53}s^3 + A_{52}s^2 + A_{51}s + A_{50};\\
A_{53} &= T_o^5 - 5T_o^4T_d + 5T_o^3T_d^2 - \frac{5}{3}5T_o^2T_d^3\\
&\quad - \frac{25}{8}T_oT_d^4 + \frac{49}{120}T_d^5;\\
A_{52} &= 5T_o^4 - 10T_o^3T_d + 5T_o^2T_d^2 + \frac{35}{6}T_oT_d^3 + \frac{17}{24}T_d^4;\\
A_{51} &= 10T_o^3 - 10T_o^2T_d - \frac{15}{2}T_oT_d^2 - \frac{5}{6}T_d^3;\\
A_{50} &= 10T_o^2 + 5T_oT_d + T_d^2/2.
\end{aligned} \tag{64}$$

From $F^n_{iyo}(s)$ it is possible to calculate $F_i(s)$ according to (20).

C. EXPERIMENTS BASED ON IPDT MODELS

Returning now to the experiments on a system with parameters (49) and a minimum filter order $n = 2$, with the time constant chosen for simplicity as $T_o = T_d$ and the gain of the feedforward and the stabilization controllers $K_P = K_p$

$$K_P = \frac{1}{eK_sT_d} \tag{65}$$

corresponding to the double real dominant closed loop pole.

The first aspect we will notice is the consideration of the constraints of the control signal. If we design the whole scheme in the linear domain and include the output limitation on the range $u \in [0, 100]$ only at the output of the controller, the transients will be with a typical over-regulation at the output (see Figure 9). To avoid overshooting due to the control saturation, according to Figure 12 in [32], the scheme with feedforward loop feedback from the output of Dynamic Saturation block might be used. However, this scheme works correctly only for $K_p = K_P$, which in our case may not be suitable, because with regard to the transmission of measurement noise we will try to reduce the value of K_p (while maintaining the loop stability) as much

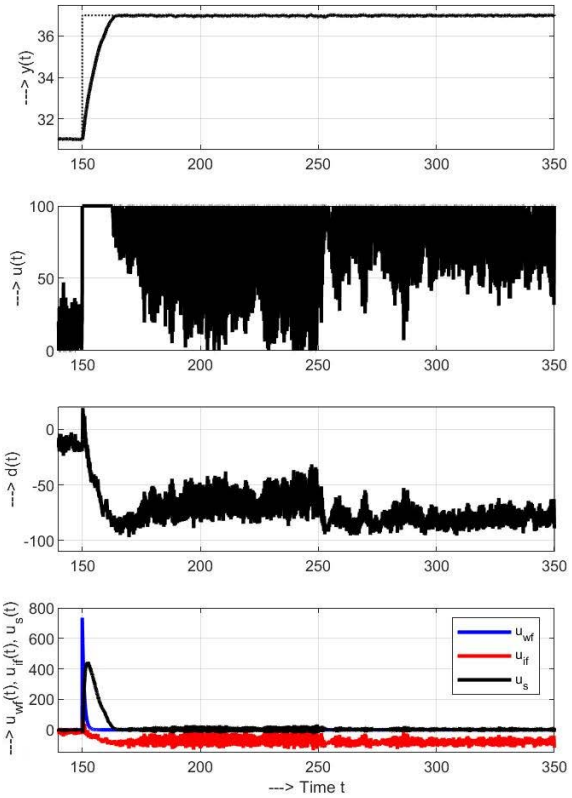

FIGURE 11. IPDT: Transients corresponding to the setpoint change from $w = 31$ to $w = 37^oC$ at $t = 150$s and to the fan voltage step from $d_i = 5$ to $d_i = 15$ at $t = 250$s; $T_o = T_d = 0.3$s; $n = 2$; $K_s = 0.01$; $K_P = K_p$ (65).

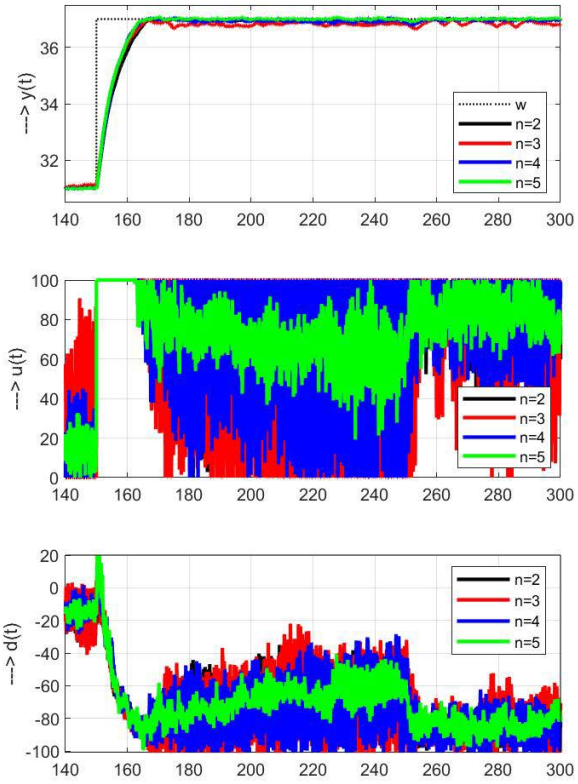

FIGURE 12. IPDT: Transients corresponding to the setpoint change from $w = 31$ to $w = 37^oC$ at $t = 150$s and to the fan voltage step from $d_i = 5$ to $d_i = 15$ at $t = 250$s; $T_d = 0.3$s; $T_o = 0.25$s; $n \in [2, 5]$; $K_s = 0.01$; $K_P = K_p$ (65).

as possible. Because when using such a scheme with $K_p < K_P$, a permanent error occurs at the output, we prefer to modify the scheme with Dynamic Saturation block according to Figure 10. In this scheme, the output from the stabilizing controller has the highest priority, which ensures monotonic responses after setpoint step changes.

Responses corresponding for $K_P = K_p$ (65) to the setpoint change from $w = 31$ to $w = 37^oC$ at $t = 150$s and to the fan voltage step from $d_i = 5$ to $d_i = 15$ at $t = 250$s in Figure 11 show a monotonic output transient to the new setpoint variable. The disturbance step caused by the fan voltage change from $d_i = 5$ to $d_i = 15$ at $t = 250$s is practically not visible in the output, just in the control signal values. Due to the inclusion of internal plant feedback in the equivalent disturbance, the reconstructed disturbance significantly changes its value after the setpoint change. Its values change even after reaching the required output, which is a manifestation of slow heat transfer by convection. Significant changes in the reconstructed disturbance occur after a change in fan power.

As it is clear from the course of the controller output u, such a nearly ideal output response was achieved by a strongly noisy controller output. It is also evident that the stabilizing controller output u_s does not completely remain at zero and, especially during the transition to the new setpoint value, it acquires considerable values. However, given the significant difference between the IPDT model used and the physical nature of the controlled process, this may not be surprising. In other words, with significant differences of the plant and model dynamics, the RM-DTC behaves the same as traditional DOB-based solutions with a stabilizing controller. In such situations RM-DTC forces, with the help of stabilizing controller, the controlled system dynamics to cope the selected model [45]. However, the RM-DTC allows the deviations between expected and actual behavior to be evaluated separately with respect to setpoint tracking, disturbance reconstruction and compensation, and overall stabilization, which can be used for more detailed analysis of system behavior and optimization of controller design.

Transients corresponding to a slightly decreased value $T_o = 0.25$s, $K_p = K_P$ (65), $n \in [2, 5]$ and with the disturbance observer and reference model tuning (63)-(64) are in Figure 12. Due to the decoupling of the setpoint and disturbance responses, the DOB filter does not significantly influence the shapes of setpoint step responses. As a result of a constant relative order of the disturbance reference model $F_i(s)$, the increase in DOB filter order n does not immediately reduce the impact of noise. Therefore, we will look for other ways to reduce the noise impact. In a nominal circuit with an integrative plant, it is sufficient for stability to work with any small positive value K_p. In the next experiment, we therefore reduce the gain of the stabilizing controller to

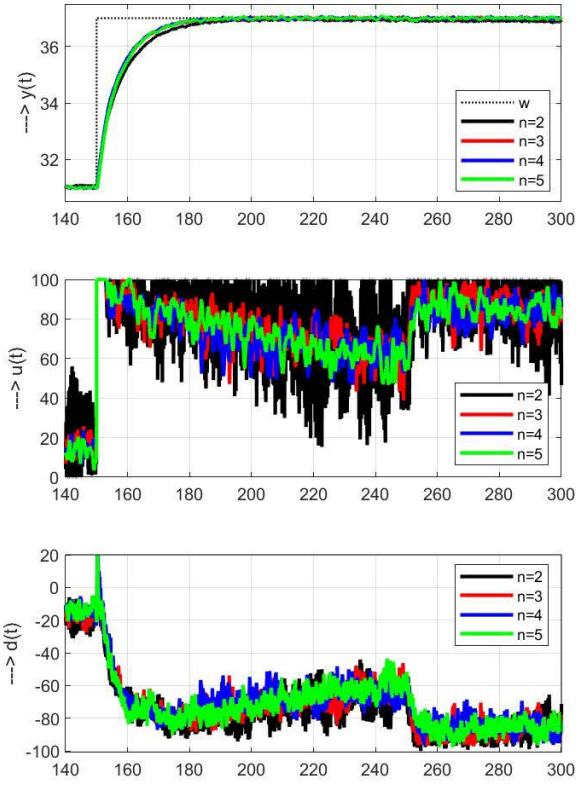

FIGURE 13. Transients corresponding to the setpoint change from $w = 31$ to $w = 37^oC$ at $t = 150s$ and to the fan voltage step from $d_i = 5$ to $d_i = 15$ at $t = 250s$; $T_d = 0.3s$; $T_o = 0.25s$; $n \in [2, 5]$; $K_s = 0.01$; $K_P = 0.1K_P$ (65).

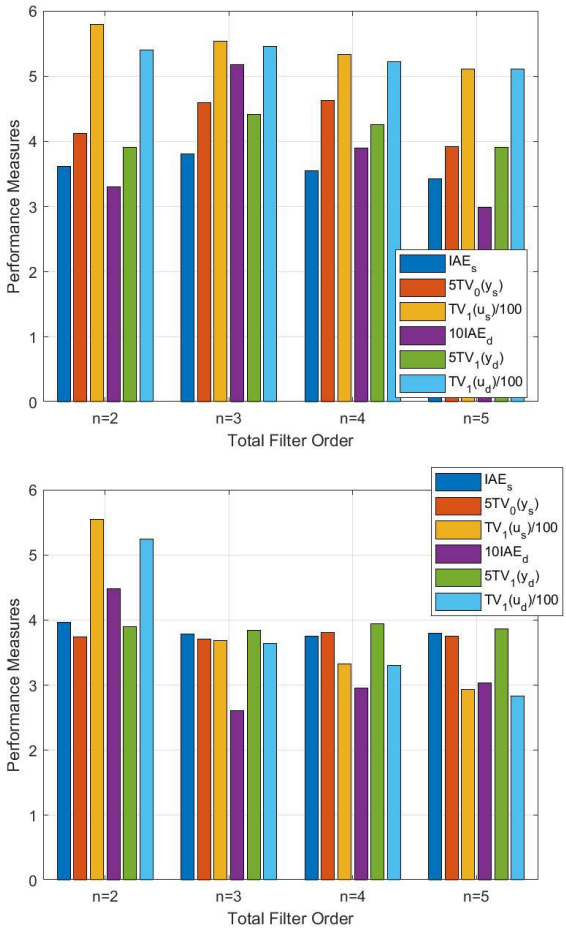

FIGURE 14. Performance measures corresponding to transients in Figure 12 (above) and (13) (below) documenting possibilities of decreasing measurement noise impact.

the value $K_p = K_P/10$. The corresponding transients on Figure 13 show that the rise of the output to the required setpoint value slowed down a bit by decreasing K_p. However, it still depends only slightly on the order of disturbance compensation filters n. A comparison of performance measures in Figure 14 shows that with the reduction of K_p, the values of IAE_s increased slightly, but all other performance values decreased significantly. A similar effect could be achieved by simplifying the disturbance reference model, in which the coefficients at higher powers would be neglected.

Remark 6 (RM-DTCs and Noise Elimination): Decoupled setpoint tracking and disturbance rejection enabled by the use of RM-DTCs focus on reducing the stabilizing controller activity by zeroing its input. This is achieved by decreasing the measured output impact by opposite expected deterministic signals added to the controller input. This is partly reminiscent of the methods known from acoustics as active noise control (ANC), noise cancellation (NC), or active noise reduction (ANR). They are reducing an unwanted permanent, or periodic sound by the addition of a second sound produced in antiphase. Although it might be interesting, we did not deal with the compensation of the effect of steady periodic signals in this work.

D. EXPERIMENTS BASED ON DIPDT MODELS

The TOM1A system can be extended to a system with dominant second-order dynamics by including an additional

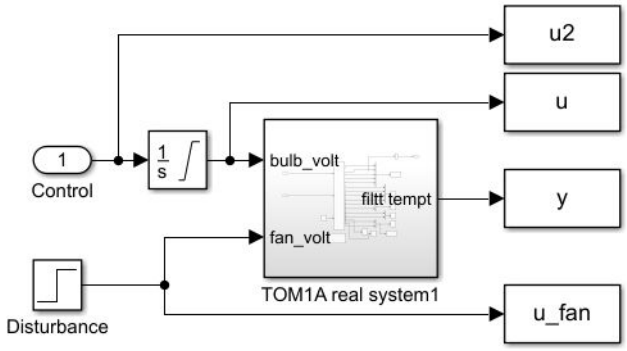

FIGURE 15. TOM1A system with integrator limited block at the input constrained to the range $u \in [0, 100]$, added to obtain a smoother bulb input signal, can be simply approximated by the DIPDT model.

integrator to the input. This, when controlled by a limited-range signal $u_2(t)$, produces a control signal $u(t)$ with the limited rate of change at its output. Of course, $u(t)$ must meet the limits of the admissible 0-100 TOM1A input range. To (at least partially) avoid the windup problem, we will use the Integrator Limited block (see Figure 15) in the

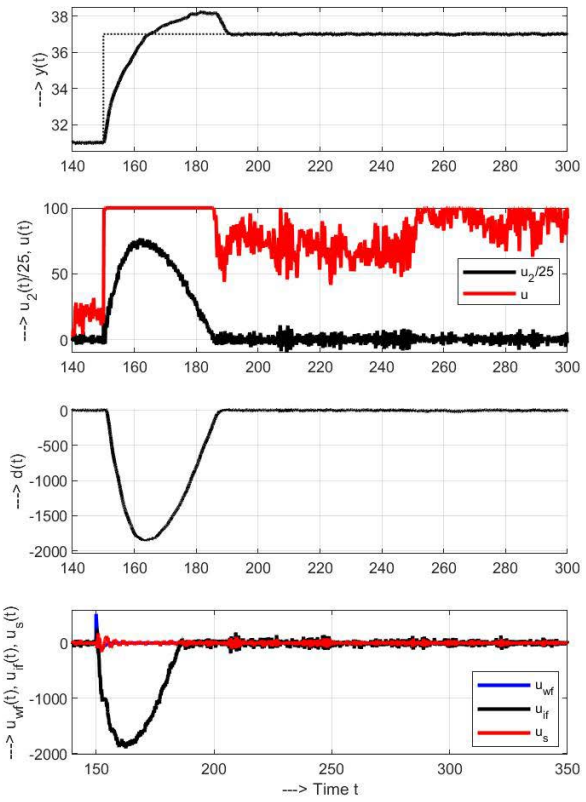

FIGURE 16. DIPDT: Transients corresponding to the Simulink model in Figure 3 with the controlled plant according to Figure 15 for the setpoint change from $w = 31$ to $w = 37^oC$ at $t = 150s$ for the fan voltage step from $d_i = 5$ to $d_i = 15$ at $t = 250s$; $T_o = 0.5s$; $T_d = 0.3s$; $n = 4$; $K_s = 0.01$; both PD controllers tuned according to (27), $T_{Df} = T_d/2$.

Matlab/Simulink program for this purpose. We will assume the system model (1) with parameters (49).

Because the output $u(t)$ of the input integrator will obviously not be affected by external influences, we will expect the values of the reconstructed disturbance to be zero at least at steady states. Thanks to the use of controllers with a derivative action, we can also expect an increased effect of measurement noise. Therefore we choose $T_o = 0.5$s.

An example of measured responses of individual variables is shown in the Figure 16. In their brief evaluation, it is necessary to mention:

1) Thanks to the use of an integrator with limited output, the course of the controlled output is overshooting. Although its shape resembles the situation in Figure 9, we now need significantly different approaches to eliminate this overshoot: limiting the signal u is actually a limitation of the state variable of the controlled second-order system. In such a situation, the parallel work of two controllers can be used by interconnecting them using the selector based ''lowest wins'' strategy [66]. In addition, when wishing to control with a limited input u_2, non-linear algorithms described e.g. in works [5], [10], [41]–[43] should be used. However, a more detailed discussion of this issue will require a separate contribution.
2) From the point of view of the design of the controller with decoupled setpoint tracking and disturbance rejection, it is important to check the output of the stabilization controller. Although it is not completely zero (due to the deviations of the model used and the actual process and measurement noise), the stabilization signal u_s is relatively small compared to the carrier signals of the design u_{wf} and u_{if}. Experiments show that u_s can be further reduced without compromising the overall stability by reducing the gains of the stabilizing regulator, which also reduces the noise level of the signals u_2 and u.
3) As we assumed, in steady states, the reconstructed disturbance is really zero and its course is completely different from the reconstructed disturbance based on the IPDT model. It is also worth noting that switching on the fan represents now, in terms of the reconstructed disturbance, a far smaller intervention than changing the setpoint.
4) In addition to the already mentioned issues concerning the elimination of output overshooting and the design of transients with rate-limited transients, it would also be interesting to test the use of higher order filters and their impact on noise attenuation and closed-loop robustness also in the case of a design based on the DIPDT model.

VI. CONCLUSION

The generalisation of the RM-DTC design methodology from the work [32], based on the IPDT models, (1) by the case of disturbance feedforward with higher order filters, (2) the case of DIPDT models and (3) the addition of experiments with real-time temperature control allowed to show the advantages and the current limitations of the methodology.

The advantages of RM -DTCs include (1) the extension of the number of degrees of freedom in controller design and (2) the decoupled design of setpoint tracking and disturbance rejection dynamics, together with (3) the modified controller structure for separate implementation of setpoint tracking and disturbance rejection control.

The introduction of a superior stabilising controller, complemented by reference models for setpoint tracking and disturbance rejection, enabled (4) the generalisation of the use of IMC structures to control unstable circuits while maintaining the reconstructed disturbance signal.

The separate evaluation of setpoint tracking and disturbance rejection together with the change of the controller signal (controller noise) opens up (5) new possibilities in terms of diagnosis, monitoring and optimisation of control loops, which is important especially with regard to fulfilling the objectives of Industry 4.0 and 5.0.

RM-DTCs are particularly suitable for (6) high-end applications with high performance and robustness requirements due to their nature. On the other hand, the structure of the

RM-DTC controller is more complex than the structure of common IMC controllers and therefore also requires a more complex control implementation for constrained processes (with input, state and output constraints), for processes with periodic disturbances, nonlinearities, etc.

(7) It is yet worth noting that the closed loop analysis based on the RM-DTC methodology can also be beneficial when finally results in using simpler controller structures.

Compared to 2DOF structures SP, which are based on the reconstruction of the output disturbance by a parallel model recalculated for an input disturbance and modified for internal stability by eliminating the reconstructed disturbance, RM-DTC seems to be more complex. Its main advantage is that the reconstructed disturbance signal is preserved. Another advantage of the proposed approach is the separation of setpoint tracking and disturbance rejection to two different branches, which are supplemented by the reference models and the stabilising controller, which simplifies the debugging and parallelization of the controller program, which can be beneficial when programming fast embedded-control based applications.

REFERENCES

[1] B. Ugurlu, M. Nishimura, K. Hyodo, M. Kawanishi, and T. Narikiyo, "Proof of concept for robot-aided upper limb rehabilitation using disturbance observers," *IEEE Trans. Human-Mach. Syst.*, vol. 45, no. 1, pp. 110–118, Feb. 2015.

[2] M. Kim, F. Beck, C. Ott, and A. Albu-Schäffer, "Model-free friction observers for flexible joint robots with torque measurements," *IEEE Trans. Robot.*, vol. 35, no. 6, pp. 1508–1515, Jul. 2019.

[3] S. Roy, I. N. Kar, J. Lee, N. G. Tsagarakis, and D. G. Caldwell, "Adaptive-robust control of a class of EL systems with parametric variations using artificially delayed input and position feedback," *IEEE Trans. Control Syst. Technol.*, vol. 27, no. 2, pp. 603–615, Mar. 2019.

[4] Y. Yuan, Y. Yu, and L. Guo, "Nonlinear active disturbance rejection control for the pneumatic muscle actuators with discrete-time measurements," *IEEE Trans. Ind. Electron.*, vol. 66, no. 3, pp. 2044–2053, Mar. 2019.

[5] I. Bélai, M. Huba, and D. Vrancic, "Comparing traditional and constrained disturbance-observer based positional control," *Meas. Control*, vol. 54, nos. 3–4, pp. 170–178, Mar. 2021.

[6] Š. Chamraz, M. Huba, and K. Žáková, "Stabilization of the magnetic levitation system," *Appl. Sci.*, vol. 11, no. 21, p. 10369, Nov. 2021.

[7] E. Sariyildiz, S. Hangai, T. Uzunovic, T. Nozaki, and K. Ohnishi, "Stability and robustness of the disturbance observer-based motion control systems in discrete-time domain," *IEEE/ASME Trans. Mechatronics*, vol. 26, no. 4, pp. 2139–2150, Aug. 2021.

[8] A. Isidori, *Nonlinear Control Systems*, 3rd ed. New York, NY, USA: Springer, 1995.

[9] C. Grimholt and S. Skogestad, "Optimal PID control of double integrating processes," *IFAC-PapersOnLine*, vol. 49, no. 7, pp. 127–132, 2016.

[10] M. Huba, Z. P. Bisták, and K. Žáková, "Predictive antiwindup PI and PID-controllers based on I_1 and I_2 models with dead time," in *Proc. 6th IEEE Medit. Conf.*, vol. 11, Jun. 1998, pp. 532–535.

[11] J. G. Ziegler and N. B. Nichols, "Optimum settings for automatic controllers," *Trans. ASME*, vol. 64, no. 11, pp. 759–768, 1942.

[12] J. Han, "From PID to active disturbance rejection control," *IEEE Trans. Ind. Electron.*, vol. 56, no. 3, pp. 900–906, Mar. 2009.

[13] R. Miklosovic and Z. Gao, "A robust two-degree-of-freedom control design technique and its practical application," in *Proc. Conf. Rec. IEEE Ind. Appl. Conf., 39th IAS Annu. Meeting.*, vol. 3, Oct. 2004, pp. 1495–1502.

[14] Z. Gao, "Active disturbance rejection control: A paradigm shift in feedback control system design," in *Proc. Amer. Control Conf.*, 2006, pp. 2399–2405.

[15] Z. Gao, "On the centrality of disturbance rejection in automatic control," *ISA Trans.*, vol. 53, no. 4, pp. 850–857, 2014.

[16] Z. Wu, Z. Gao, D. Li, Y. Chen, and Y. Liu, "On transitioning from PID to ADRC in thermal power plants," *Control Theory Technol.*, vol. 19, no. 1, pp. 3–18, Feb. 2021.

[17] S. Zhao and Z. Gao, "Modified active disturbance rejection control for time-delay systems," *ISA Trans.*, vol. 53, no. 4, pp. 882–888, Jul. 2014.

[18] S. Chen, W. Xue, S. Zhong, and Y. Huang, "On comparison of modified ADRCs for nonlinear uncertain systems with time delay," *Sci. China Inf. Sci.*, vol. 61, no. 7, p. 70223, Jul. 2018.

[19] M. Fliess and C. Join, "Model-free control," *Int. J. Control*, vol. 86, no. 12, pp. 2228–2252, 2013.

[20] N. Jiang, S. Zhang, J. Xu, and D. Zhang, "Model-free control of flexible manipulator based on intrinsic design," *IEEE/ASME Trans. Mechatronics*, vol. 26, no. 5, pp. 2641–2652, Oct. 2021.

[21] A. Feldbaum, *Optimal Control Systems*. New York, NY, USA: Academic, 1965.

[22] J. Mao, H. Tachikawa, and A. Shimokohbe, "Double-integrator control for precision positioning in the presence of friction," *Precis. Eng.*, vol. 27, no. 4, pp. 419–428, Oct. 2003.

[23] G. A. Hassaan, "Controller tuning for disturbance rejection associated with delayed double integrating processes: Part I: PD-PI controller," *Int. J. Comput. Techn.*, vol. 2, no. 3, pp. 110–115, 2015.

[24] M. Huba and D. Vrančić, "Delay equivalences in tuning PID control for the double integrator plus dead-time," *Mathematics*, vol. 9, no. 4, p. 328, Feb. 2021.

[25] H. S. Lee and M. Tomizuka, "Robust motion controller design for high-accuracy positioning systems," *IEEE Trans. Ind. Electron.*, vol. 43, no. 1, pp. 48–55, Feb. 1996.

[26] H. Kobayashi, S. Katsura, and K. Ohnishi, "An analysis of parameter variations of disturbance observer for motion control," *IEEE Trans. Ind. Electron.*, vol. 54, no. 6, pp. 3413–3421, Dec. 2007.

[27] M. Ruderman, M. Iwasaki, and W.-H. Chen, "Motion-control techniques of today and tomorrow: A review and discussion of the challenges of controlled motion," *IEEE Ind. Electron. Mag.*, vol. 14, no. 1, pp. 41–55, Mar. 2020.

[28] E. Sariyildiz, R. Oboe, and K. Ohnishi, "Disturbance observer-based robust control and its applications: 35th anniversary overview," *IEEE Trans. Ind. Electron.*, vol. 67, no. 3, pp. 2042–2053, Mar. 2020.

[29] J. M. Smith, "Closer control of loops with dead time," *Chem. Eng. Prog.*, vol. 53, no. 5, pp. 217–219, 1957.

[30] M. Huba, P. Bisták, and D. Vrančić, "2DOF IMC and smith-predictor-based control for stabilised unstable first order time delayed plants," *Mathematics*, vol. 9, no. 9, p. 1064, May 2021.

[31] M. Huba, P. Bisták, D. Vrančić, and K. Zakova, "Dead-time compensation for the first-order dead-time processes: Towards a broader overview," *Mathematics*, vol. 9, no. 13, p. 1519, Jun. 2021.

[32] M. Huba, P. Bistak, D. Vrancic, and K. Zakova, "Asymmetries in the disturbance compensation methods for the stable and unstable first order plants," *Symmetry*, vol. 12, no. 10, p. 1595, Sep. 2020.

[33] Q.-C. Zhong and J. E. Normey-Rico, "Control of integral processes with dead-time. Part 1: Disturbance observer-based 2DOF control scheme," *IEE Proc., Control Theory Appl.*, vol. 149, no. 4, pp. 285–290, Jul. 2002.

[34] J. E. Normey-Rico and E. F. Camacho, "Dead-time compensators: A survey," *Control Eng. Pract.*, vol. 16, no. 4, pp. 407–428, Apr. 2008.

[35] J. E. Normey-Rico and E. F. Camacho, "Unified approach for robust dead-time compensator design," *J. Process Control*, vol. 19, no. 1, pp. 38–47, Jan. 2009.

[36] B. C. Torrico, M. U. Cavalcante, A. P. S. Braga, J. E. Normey-Rico, and A. A. M. Albuquerque, "Simple tuning rules for dead-time compensation of stable, integrative, and unstable first-order dead-time processes," *Ind. Eng. Chem. Res.*, vol. 52, no. 33, pp. 11646–11654, Jul. 2013.

[37] R. C. S. Rodrigues, A. K. R. Sombra, B. C. Torrico, R. D. O. Pereira, M. D. D. N. Forte, M. P. D. A. Filho, and F. G. Nogueira, "Tuning rules for unstable dead-time processes," *Eur. J. Control*, vol. 59, pp. 250–263, May 2021.

[38] M. Iwasaki, K. Seki, and Y. Maeda, "High-precision motion control techniques: A promising approach to improving motion performance," *IEEE Ind. Electron. Mag.*, vol. 6, no. 1, pp. 32–40, Mar. 2012.

[39] M. Huba and D. Vrančić, "Delay equivalences in tuning PID control for the double integrator plus dead-time," *Mathematics*, vol. 9, no. 4, p. 328, Feb. 2021.

[40] A. Visioli, *Practical PID Control*. London, U.K.: Springer, 2006.

[41] M. Huba and P. Bistak, "Dynamic classes in the PID control," in *Proc. Amer. Control Conf.*, vol. 6, San Diego, CA, USA, 1999, pp. 3868–3872.

[42] P. Bisták and M. Huba, "Model reference control of a two tank system," in *Proc. 18th Int. Conf. Syst. Theory, Control Comput. (ICSTCC)*, Sinaia, Romania, Oct. 2014, pp. 952–957.
[43] M. Huba, P. Bisták, and I. Bélai, "Comparing constrained model based controllers for nonlinear hydraulic plant," *IFAC-PapersOnLine*, vol. 48, no. 29, pp. 283–288, 2015.
[44] Q.-C. Zhong and L. Mirkin, "Quantitative analyses of robust stability region and disturbance response of processes with an integrator and long dead-time," in *Proc. 40th IEEE Conf. Decis. Control*, Orlando, FL, USA, Dec. 2001, pp. 1861–1866.
[45] E. Schrijver and J. van Dijk, "Disturbance observers for rigid mechanical systems: Equivalence, stability, and design," *J. Dyn. Syst., Meas., Control*, vol. 124, no. 4, pp. 539–548, Dec. 2002.
[46] M. Huba and S. Kozák, "From e-Learning to industry 4.0," in *Proc. Int. Conf. Emerg. eLearning Technol. Appl. (ICETA)*, 2016, pp. 103–108.
[47] S. Vaidya, P. Ambad, and S. Bhosle, "Industry 4.0—A glimpse," *Proc. Manuf.*, vol. 20, pp. 233–238, Jan. 2018.
[48] M. Huba, "Robust controller tuning for integral dead time systems," *IFAC Proc. Volumes*, vol. 43, no. 21, pp. 218–225, 2010.
[49] M. Huba, J. Škrinárová, and P. Bisták, "Higher order PD and iPD controller tuning," *IFAC-PapersOnLine*, vol. 53, no. 2, pp. 8808–8813, 2020.
[50] S. Skogestad, "Simple analytic rules for model reduction and PID controller tuning," *J. Process Control*, vol. 13, no. 4, pp. 291–309, Jun. 2003.
[51] I. Bélai, M. Huba, K. Burn, and C. Cox, "PID and filtered PID control design with application to a positional servo drive," *Kybernetika*, vol. 55, no. 3, pp. 540–560, Sep. 2019.
[52] M. Huba and D. Vrančić, "Extending the model-based controller design to higher-order plant models and measurement noise," *Symmetry*, vol. 13, no. 5, p. 798, May 2021.
[53] M. Hypiusová and D. Rosinová, "Discrete-time pole-region robust controller for magnetic levitation plant," *Symmetry*, vol. 13, no. 1, p. 142, Jan. 2021.
[54] Y. Sueki and Y. Noda, "Experimental verification of real-time flow-rate estimations in a tilting-ladle-type automatic pouring machine," *Appl. Sci.*, vol. 11, no. 15, p. 6701, Jul. 2021.
[55] V. G. Rao and D. S. Bernstein, "Naive control of the double integrator," *IEEE Control Syst.*, vol. 21, no. 5, pp. 86–97, Oct. 2001.
[56] M. Vítečková and A. Víteček, "2DOF PI and PID controllers tuning," in *Proc. 9th IFAC Workshop Time Delay Syst.*, vol. 9, Prague, Czech Republic, 2010, pp. 343–348.
[57] M. Viteckova and A. Vitecek, "2DOF PID controller tuning for integrating plants," in *Proc. 17th Int. Carpathian Control Conf. (ICCC)*, May 2016, pp. 793–797.
[58] K. J. Åström and T. Hägglund, *Advanced PID Control*. Research Triangle Park, NC, USA: ISA, 2006.
[59] M. Č. Bošković, T. B. Šekara, and M. R. Rapaić, "Novel tuning rules for PIDC and PID load frequency controllers considering robustness and sensitivity to measurement noise," *Int. J. Electr. Power Energy Syst.*, vol. 114, Jan. 2020, Art. no. 105416.
[60] M. Huba, D. Vrančić, and P. Bisták, "PID control with higher order derivative degrees for IPDT plant models," *IEEE Access*, vol. 9, pp. 2478–2495, 2021.
[61] X.-Y. Lu and S. K. Spurgeon, "Robust sliding mode control of uncertain nonlinear systems," *Syst. Control Lett.*, vol. 32, no. 2, pp. 75–90, Nov. 1997.
[62] H. Han, X. Wu, and J. Qiao, "Design of robust sliding mode control with adaptive reaching law," *IEEE Trans. Syst., Man, Cybern., Syst.*, vol. 50, no. 11, pp. 4415–4424, Nov. 2020.
[63] M. Huba, Š. Chamraz, P. Bisták, and D. Vrančić, "Making the PI and PID controller tuning inspired by Ziegler and Nichols precise and reliable," *Sensors*, vol. 21, no. 18, p. 6157, Sep. 2021.
[64] M. Huba, P. M. Oliveira, P. Bisták, D. Vrančić, and K. Žáková, "A set of active disturbance rejection controllers based on integrator plus dead-time models," *Appl. Sci.*, vol. 11, no. 4, p. 1671, Feb. 2021.
[65] T. Huba, M. Huba, P. Ťapák, and P. Bisták, "New thermo-optical plants for laboratory experiments," in *Proc. IFAC World Congr.*, Cape Town, South Africa, 2014, pp. 1–6.
[66] A. Glattfelder and W. Schaufelberger, *Control Systems With Input and Output Constraints*. Berlin, Germany: Springer, 2003.

MIKULAS HUBA (Member, IEEE) received the M.Sc. and Ph.D. degrees in technical cybernetics, in 1974 and 1982, respectively. From 1996 to 2008, he was the Head of the University Distance Education Centre. From 2008 to 2011, he was a Researcher and a Mercator Visiting Professor with FernUniversität Hagen, Germany. From 2015 to 2019, he was the Director of the Institute of Automotive Mechatronics. Since 2008, he has been a Full Professor with the Faculty of Electrical Engineering and Information Technology, STU in Bratislava. From 2013 to 2021, he was the Head of the Department of E-mobility, Drives, and Automation. He is the author and coauthor of about 400 papers in journals and proceedings of international conferences, 20 monographs on constrained, nonlinear and remote control, about e-learning, and organizer of 11 international conferences Virtual University and other IFAC and IEEE events.

DAMIR VRANCIC is currently working as a Senior Research Fellow with the Department of Systems and Control, Jožef Stefan Institute, Ljubljana. In the field of controller parameter tuning, he has developed novel methods of parameter tuning, based on time and frequency response of the process. In the field of adaptive systems, he with his colleagues have developed and patented an adaptive system for the manipulation of dynamic gain of a valve drive to adaptively suppress oscillations. His research interests include controller tuning (PID controllers, multivariable controllers, cascade loops and Smith predictors), anti-windup, adaptive systems, and electronics.

PAVOL BISTAK received the M.Sc. degree in technical cybernetics and the Ph.D. degree in automation and control, in 1988 and 2013, respectively. He has been a University Teacher and a Researcher with the Faculty of Electrical Engineering and Information Technology, Slovak University of Technology in Bratislava, since 1992. He has been the Head of the Department of E-mobility, Drives, and Automation, since 2021. He is the author or coauthor of more than 130 articles in journals, conference proceedings, textbooks, or book chapters. His research interests include nonlinear control systems and new technologies in education. In recent years, his field of interests include the design of PID controllers, the design of mechatronic systems, and the IoT.